Application of the 3D Limit Equilibrium Method for Slope Stability Analysis at the Bingham Canyon Mine, A Case Study

Jeffrey Telfer *Rio Tinto, Salt Lake City, USA*

Forrest Schumacher *Rio Tinto, Salt Lake City, USA*

Abstract

In June 2019, the geotechnical engineering team at Rio Tinto Kennecott's (RTK) Bingham Canyon Mine detected elevated slope movement in the mine's East wall through its extensive network of surface and subsurface monitoring systems. The deformation area (called the Upper Ohio) had a slope height of approximately 1,200 ft and an estimated tonnage of approximately 4.6 MTons. A detailed slope stability evaluation was initiated to understand the instability mechanism and investigate of mitigation options. The geotechnical team conducted an extensive and focused characterization of the Upper Ohio and developed 3D limit equilibrium models to back-analyze the wall movement and run predictive cases to guide management decision. This case study presents the analysis undertaken at RTK to evaluate the risk of the instability. As this was the first major 3D limit equilibrium model generated by in-house RTK geotechnical engineers, key learnings are also presented.

1 Introduction

Three-dimensional (3D) slope stability modelling has typically been considered a speciality often outsourced to consultants rather than executed by in-house geotechnical teams. This is in some part due to the complexity of the modelling software and the limited capacity of in-house teams to dedicate resources to the fluctuating demands of this work. However, as software is introduced that reduces the modelling complexity and is easier to operate (specialist coding vs. graphical user interface), the opportunity for in-house geotechnical engineers to execute this analysis in shorter timeframes increases (McQuillan et al., 2020, Bar et al., 2019).

The geotechnical team at Rio Tinto Kennecott (RTK) have undertaken several 3D slope stability investigations with both limit equilibrium (LE) and numerical approaches. This paper explores a case study of applying 3D LE analysis to a wall area showing elevated movement to assist with slope stability management.

2 Geological Setting

The Bingham Canyon Mine is a porphyry Cu-Mo-Au deposit in the Oquirrh Mountains, southwest of Salt Lake City near the eastern margin of the Basin and Range province. The Oquirrh Mountains are predominantly mid- to late Paleozoic siliciclastic and carbonate sedimentary rocks disrupted by the mid-Eocene intrusion of monzonite and successive porphyry intrusions (Porter et al., 2012).

The sedimentary units were folded and faulted through multiple events including thrusting, extension, relaxation, and intrusion. Prominent bedding parallel faults exist throughout the quartzite and limestone units, particularly at the contacts between these two rock types, with kinematic indications of thrust and normal movement in the fault fabrics. These faults vary in thickness and infill material between different horizons and along the fault length itself.

The Upper Ohio instability is a multi-bench wall movement occurring along a named bedding fault called the Pepperpike, with a side-release along persistent orthogonal joint sets. Monitoring data indicated the height of the instability to be around 1,200 ft with an estimated tonnage of approximately 4.6MTons (Figure 1). The location of the instability is within the Upper Ohio quartzite domain of the East wall (Figure 2), where bedding dips from high 30°'s to low 40°'s, striking greater than 50° oblique to the wall orientation. This area is within a mining cutback where high mining rates leads to faster bench turnovers, and in turn an elevated response of the slope to toe mining activities.

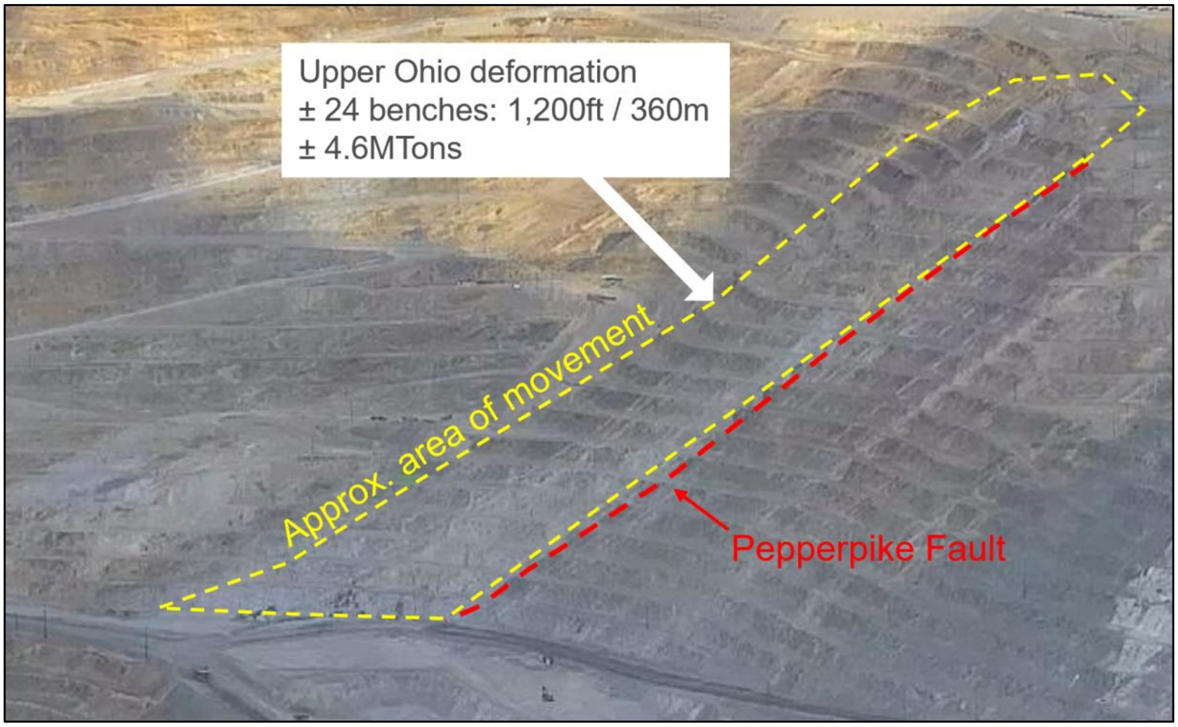

Figure 1. Bingham Canyon Mine camera view of Upper Ohio deformation in 2019.

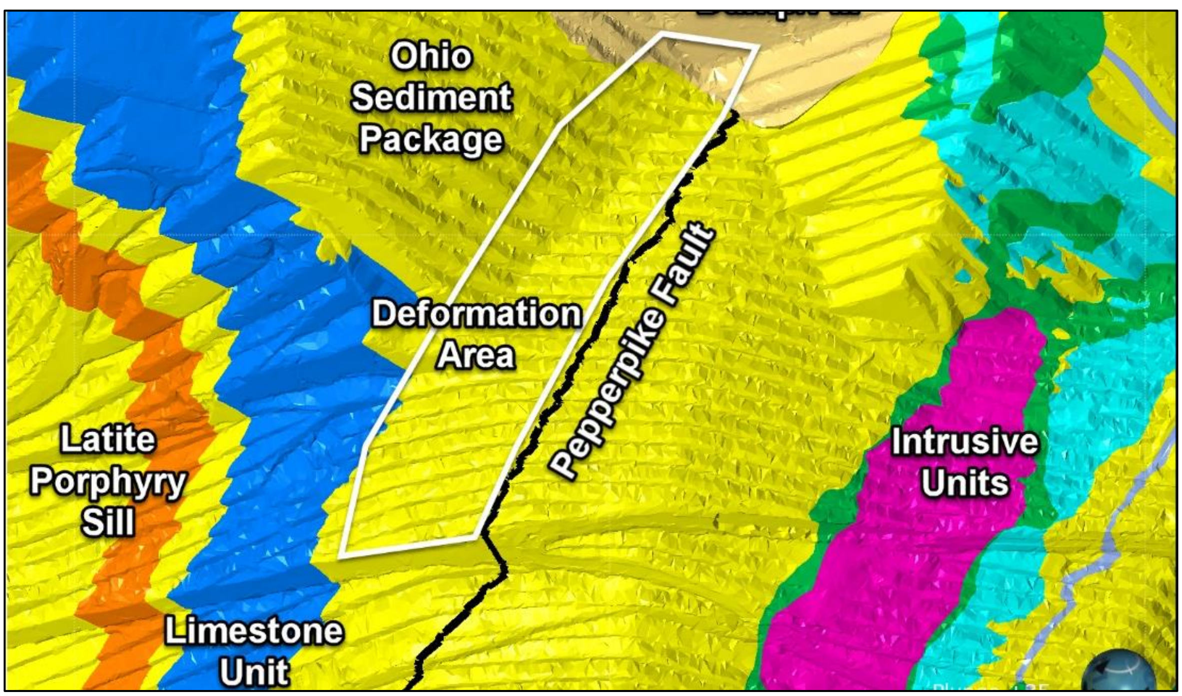

Figure 2. 3D model view of Upper Ohio area geologic setting looking Southeast

3 Monitoring data

Upper Ohio slope movement was detected by multiple slope monitoring methods deployed at the mine, including ground-based radars (RAR and SAR), prisms, GPS units, and InSAR. Following surface detection, subsurface instrumentation consisting of TDR’s and inclinometers employed in boreholes also detected shearing below ground on the Pepperpike fault. Tension cracks on the crest of the movement were also measured and monitored with extensometers.

Field observations included the following:

- The lower slope was more responsive than the upper slope to toe mining activities across the controlling fault mechanism (Pepperpike).
- Blasting and excavation in the immediate toe on the hanging wall side of the fault caused an immediate slope response.
- Pausing mining activities in the toe reduced rate of slope deformation. Detailed slope monitoring review was completed during mining pauses.
- Clay gouge infill was observed in the Pepperpike fault throughout the lowest benches of deformation.
- The wall was observed to be dry in the upper benches of the slope and sub-surface vibrating wire piezometers did not indicate pore pressures in the movement area.

Figure 3 shows a displacement map and live time series of the Upper Ohio area of deformation in response to toe mining activities. Negative deformation indicates movement out of the slope (i.e. towards the radar unit). Jumps in the time series data indicating movement into the slope (away from the radar) are likely due to atmospheric or mining equipment noise. Figure 4 presents GPS locations through the Upper Ohio area of deformation, their trend direction of movement, and displacement magnitude. A rapid acceleration period is clearly observed in this GPS data in March/April 2020.

Overall levels of movement, location relative to critical infrastructure (haul road) and ore, consistent deformation trends, and high sensitivity to toe mining activity called for in-depth geotechnical characterization and creation of a stability model to establish whether the mining cut could be continued without a slope failure.

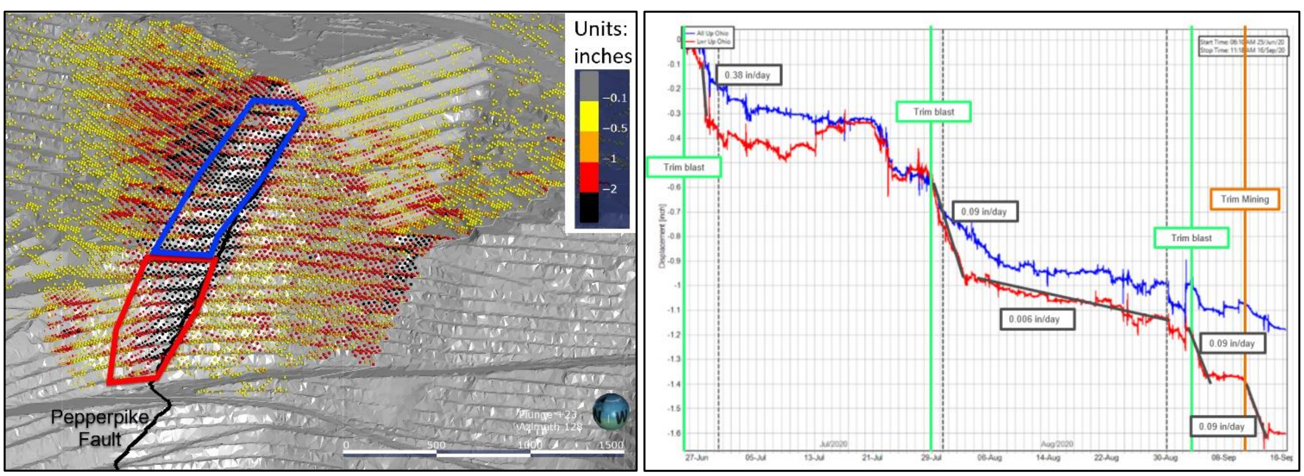

(3a) (3b)

Figure 3a and 3b. Displacement map (3a) and live synthetic aperture radar time series data (3b) of the Upper Ohio area of deformation for the period of end of June 2020 to mid-September 2020. Events for trim blasting and mining are shown to highlight the mining response. The colors of the area outlines in Figure 3a correspond to the color shown in the radar displacement time series in Figure 3b.

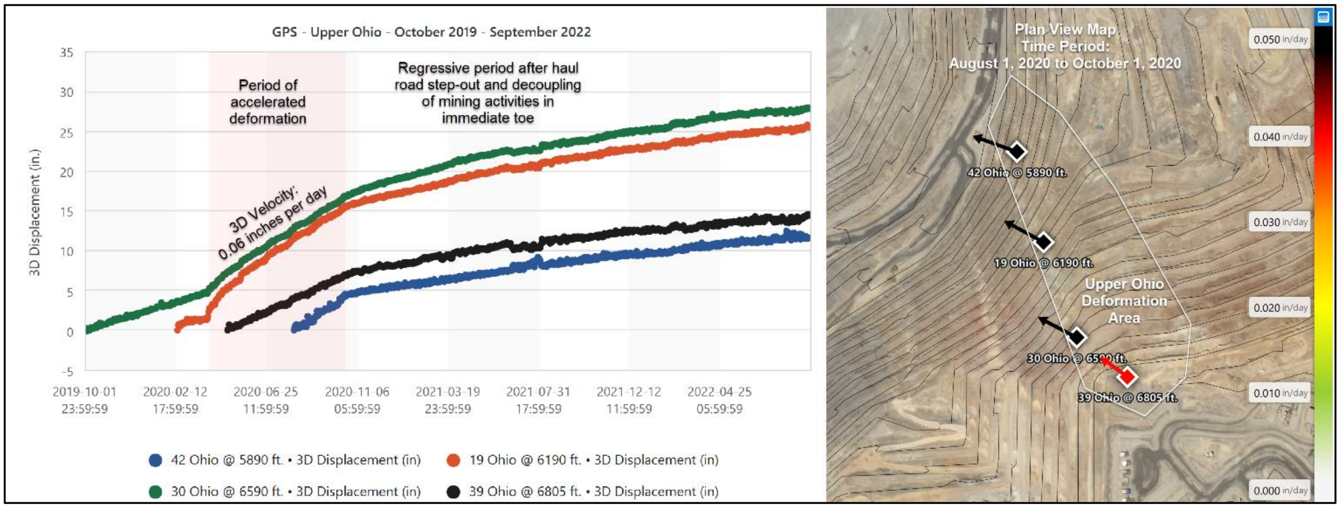

Figure 4. Upper Ohio GPS 3D displacement trends, October 2019 to September 2022 (time series) and August 2020 to October 2020 (plan view map of GPS trends). GPS unit numbers in the plot correspond to the same numbers in the plan view map.

4 Engineering Geology

Early detection of slope movement within the Upper Ohio in 2020 initiated an in-house review of rock mass, structural geology, and hydrogeological conditions to develop a full understanding of the failure mechanism. Georeferenced radar data was draped over drone flights and geologic models to determine extent of movement. Detailed field and drone flight mapping together with drillhole and televiewer data review provided the following findings:

- Right side controlled by the Pepperpike bedding fault, which had previously been involved in small-scale wedge crest failures in consecutive benches.
- Pepperpike fault is continuous along the full slope height of 1200 ft and was found to be steeper than originally anticipated; it was subsequently re-modeled incorporating the field data.
- The orientation of the Pepperpike ranged from 30-40˚ dip and a dip direction 0-10˚ relative to mine grid north. Dip direction relative to the slope orientation proved critical.
- Pepperpike fault infill consisted of weak clay gouge towards the bottom half of the slope.
- GSI of quartzites estimated from field mapping between 32-35 with persistent bedding orthogonal joint sets (frictional infill) of at least full bench height length (50 ft).

Three (3) different strength characteristics were identified along the fault length, consisting of zones of general bedding fabric (minimal infilling), non-gouge (silty/sandy frictional infilling) and gouge (weak clay-rich infilling). Figure 5 shows the variation of the modeled Pepperpike fault between 2018 and 2020. There was strong relation between higher levels of deformation in the monitoring data to the location of the gouge zone (Figure 6), and strong evidence of slickensides in this zone.

Further to this, targeted geotechnical cell mapping was undertaken on the bounds of the wall movement area to investigate the rock mass conditions; results and observations from this mapping are shown in Figure 7. Cells mapped on the right bound clearly identified the Pepperpike fault as a 10-inch to 12-inch thick clay gouge unit with some differential displacement across the fault zone. Cells mapped to left of the wall movement area showed a persistent joint set orthogonal to bedding spanning entire 50 ft bench height. The left-hand bound of the movement area wrapped slightly around a corner in the pit design, indicating that a reduction in confinement that the corner created could be a contributing factor.

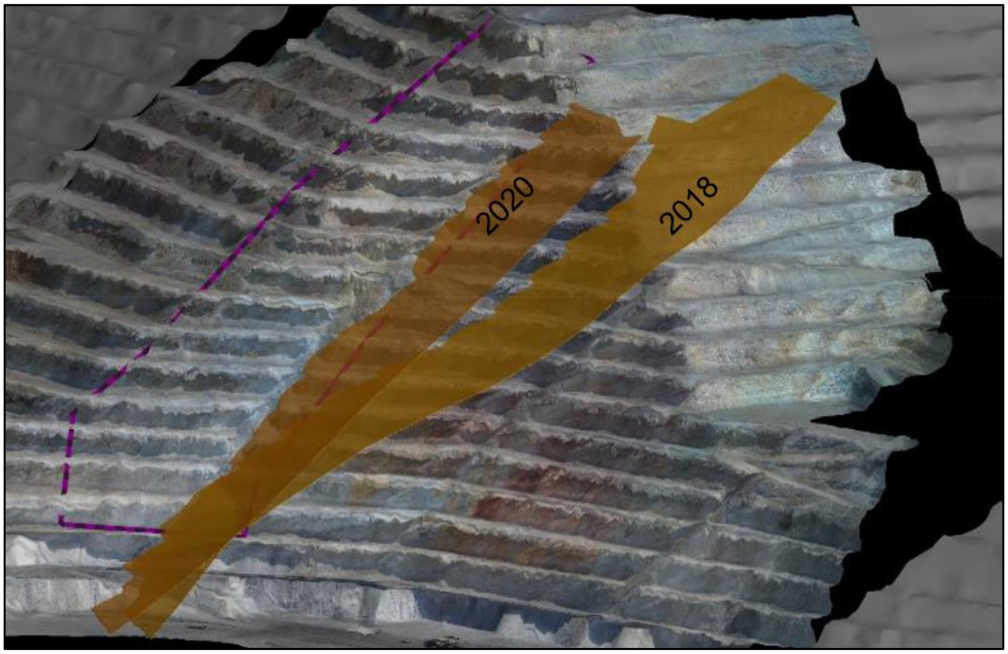

Figure 5. Variation of Pepperpike fault model. The 2018 version of the fault was used in original geotechnical stability modeling of the area. The steeper dipping 2020 version was updated in the 3D models described in this case study.

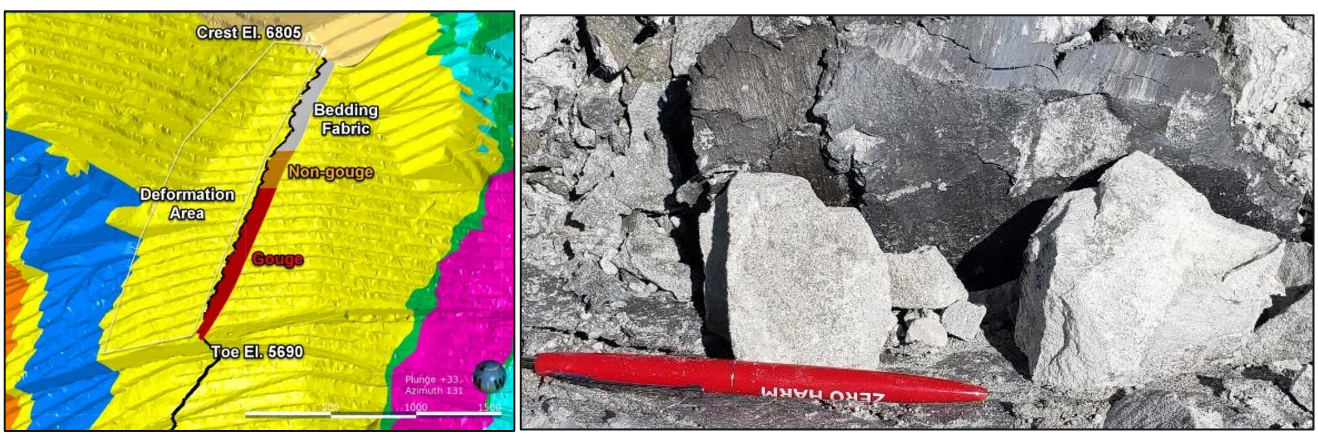

Figure 6. Characterized zones of the Pepperpike Fault infill properties and photograph of the clay gouge found on the fault surface.

In addition to targeted cell mapping, a structural mapping data set from geological and geotechnical mapping in the area was interrogated (Figure 8). This data set captures both the major structures and joint fabric. From a simple kinematics perspective, the stereonet shows how the combination of this orthogonal joint set with the bedding dip creates a daylighting wedge-type mechanism with the pit orientation in this wall sector.

Figure 7. Targeted geotechnical cell mapping observations with the left insert showing the orthogonal joint sets and the right insert showing the Pepperpike fault.

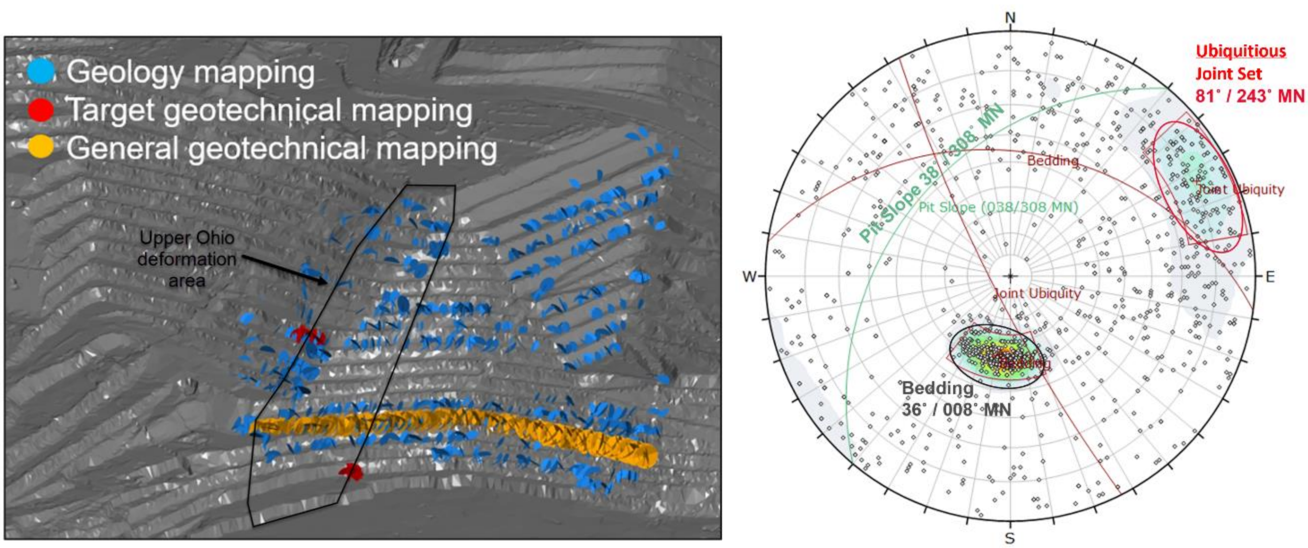

Figure 8. Locations of structural orientation picks and stereonet of general rock fabric in the area of the Upper Ohio. This stereonet shows the major bedding orientation along with the persistent orthogonal to bedding joint set involved in the mechanism. The two (2) sets form a daylighting wedge on the inter-ramp scale.

5 3D stability modelling discussion

With an understanding of the general character and mechanism of the Upper Ohio instability, it was decided that a stability model would be valuable for managing the wall going forward. The kinematic-style mechanism identified in the structural assessment lends itself well to LE analysis. Given the wedge characteristic, as well as a change in wall orientation in this area, 3D analysis was required to capture the relative orientations of structural features and wall orientation to define the slip surface more accurately.

Read & Stacey (2009) and Read (2020) discuss the merits of LE and numerical modelling methods and suggest that numerical methods should only be considered where their sophisticated nature of analysis will bring necessary added value. Often the results from LE analysis are perfectly adequate to inform decisions (Read & Stacey 2009). Further to this, the complexity of numerical methods calls on high confidence in input data (Read & Stacey 2009), with a longer model build and run times (Kabuya et al., 2020). Time is often limited when analyzing a developing instability. LE models are widely chosen for mine slope stability analysis due to relatively straightforward model development and rapid computation times (Kabuya et al. 2020, Bar et al. 2019).

Although 3D LE analyses appeared in literature in the 1960's (Read, 2020) and software has been available for nearly a decade, its application in the industry is not yet commonplace, with 2D assessment being carried out more regularly even where failure mechanisms have a three-dimensional nature (McQuillan et al., 2020). Read (2021) raises concerns about the fundamentals of 3D LE modelling, the relativity of 2D and 3D Factor of Safety ("FS") results to each other, and the variability in 3D LE FS values between different software packages. The authors of this paper acknowledge these points. For this case study, a key component of the application of 3D LE analysis was the comparative nature of determining relative difference between a back analyzed model and predictive cases. Substantial value can be gained from comparing relative difference if the model is respecting the understood mechanism of failure.

Numerical methods of stability analysis were considered for this problem, however given the features of this instability and project needs, it was determined that a 3D LE model would provide valuable results in an adequate timeframe for the operation.

6 Back analysis

Back analysis was undertaken using Slide 3D (Rocscience). The goal of the 3D LE model was to back analyze the instability and model a slip surface that respected the understood mechanism, with a target factor of safety (FS) between 1.0-1.1 representing the marginal stability condition indicated by the monitoring data.

6.1 Input Parameters

Initial rock mass and defect properties were taken from already existing feasibility level studies for the design of the pit wall. The instability sits within the Upper Ohio quartzites, and this rock unit was further sub-domained based on the natural weathering horizon separating an upper weaker zone from the lower quartzite unit. Table 1 summarizes the initial Mohr-Coulomb defect strengths and Table 2 summarizes the initial Hoek-Brown rock mass parameters for these units. As discussed above, the instability characterization resulted in a refined structural geology model consisting of a new Pepperpike fault surface with updated fault strength zones (gouge, non-gouge and bedding), and ubiquitous anisotropic defect sets for bedding and the orthogonal joints. Groundwater observations from mining and sub-surface monitoring indicated that this area was dry.

Table 1. Discontinuity/defect and Fault Strengths (Mohr-Coulomb)

Unit/Type	Friction angle (°)	Cohesion (psi)
Pepperpike Gouge	16	7
Pepperpike Non-Gouge	28	4
Pepperpike Bedding Fabric	30	28
Left release orthogonal joint set	29	0

Table 2. Rock Mass strength parameters for Generalized Hoek Brown inputs

Rock Mass	***GSI***	***mi***	***UCS (psi)***	***Disturbance factor***
Quartzite (Weak Zone - weathering)	25	15	1,885	0.7
Quartzite	31	15	4,931	0.7

Nominal values based on literature were initially used for the anisotropic linear strength assignment parameters (A and B angles). The A angle defines the angular range away from the bedding orientation for which the defect strengths apply on a slip surface, while the B angle defines an angular range through which the material strength transitions from defect to rock mass strength (Rocscience, 2022). Bar and Weekes (2017) state that A=5° is commonly adopted in industry with justification based on general variability in the geological model, accuracy of geological mapping compasses and the resolution of slip surfaces in LE software. With A set to 5° as a starting point, an initial value of B=6° was selected representing a relatively sharp transition from rock mass to defect strength. Transitional strengths between rock mass and defects was not considered critical to this investigation.

6.2 Model Iterations

Initial models with base-case material strengths gave a nonrepresentative failure shape and an FS>1.3, too high for an instability back analysis. To better replicate the failure shape showing on monitoring data, initial refinements of the back analysis model were focussed on the structural geological controls. In subsequent steps, the material strengths were reduced to bring the stability margin closer to a target FS between 1.0-1.1 (being cognisant that reducing material strengths has the potential to realise a different mechanism).

On review of the wall mapping dataset, when removing the bedding records from the stereonet it became apparent that the orthogonal joint set exhibits a strong concentration at orientation 81°/243° (Dip/DDR) and a secondary joint cluster of similar dip but with a more westerly dip direction (77°/269°), see Figure 9. So, with the curiosity that a back analysis assessment requires, a trial was run incorporating both joint sets. This stereonet was also used to refine the A angle for anisotropic linear strength assignment. Evidence on the stereonet in Figure 9 supports a 10° A angle shown by the circles encompassing the joint clusters, so the A angle was increased to 10°, and following suit, the B angle was updated to 11°. Bar and Weekes (2017) state that 10° for an A angle is justifiable for highly variable joint orientations.

The interaction between the two joint sets with the updated A and B angles resulted in a more representative failure shape, indicating that the primary joint set was perhaps not a critical set. Using only the primary joint set did not allow the model to capture the required step-path side-release. One could increase A angle to allow more structural orientation variability however this would have falsely introduced shallower and steeper dipping structures that don't present on the stereonet. Adding a second ubiquitous set allows more dip directional variability whilst respecting the dip range of the data. The global minimum FS of this model was still high at FS=1.3 (Figure 10), and so further refinement of material strengths was required. The modeled slip surface did however find the correct mechanism, which consisted of the Pepperpike as the right release surface, the left release as the orthogonal joint set, and rock mass at the toe.

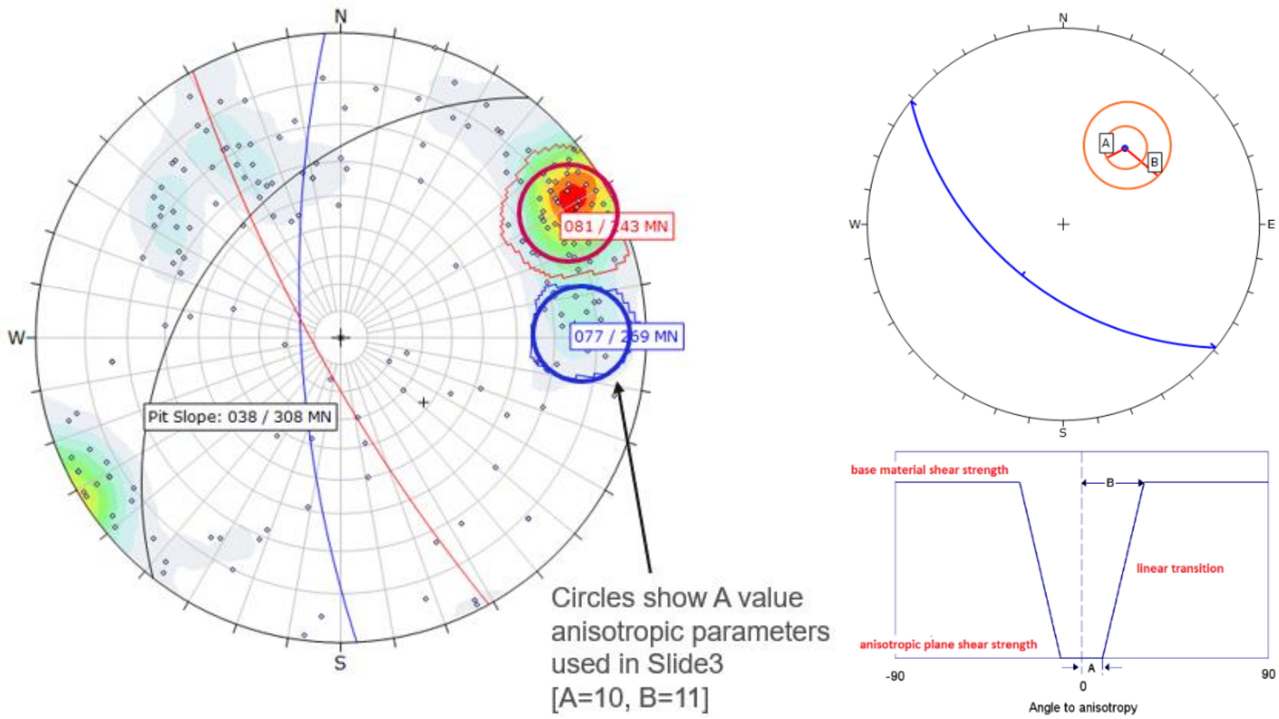

Figure 9. Structural orientations depicted on a stereonet of the input parameters for the Generalized Anisotropic strength for the Upper Ohio Slide3 model (adapted from Rocscience, 2022).

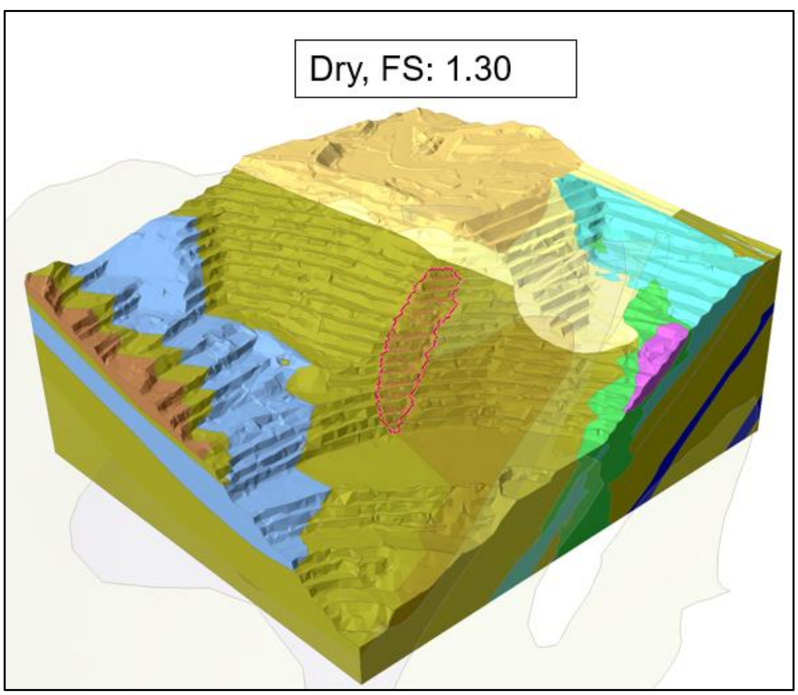

Figure 10. Initial results of the first back analysis iteration assuming a dry slope and base case rock mass and discontinuity strengths. FS of 1.30 was too high for a back analysis.

The iterative back analysis process of reducing material strengths to achieve stability margins that reflect field performance in the Upper Ohio required changes to both rock mass and defect strengths. The rock mass strength was reduced by increasing the D factor from 0.7 to 0.9 to account for increased disturbance associated with wall movement and to represent the history of wall sensitivity to blasting. Defect strengths were reduced through the removal of cohesion from non-gouge fault, bedding fault and bedding and joint anisotropy given the mobilization and likely dilation of the wall. Cohesion remained unchanged in the gouge bedding fault unit since this zone had high clay content. With these changes the global minimum FS dropped down to 1.13 with a mechanism that respected the monitoring data and geological understanding.

Although subsurface monitoring and surface observations up until this time had indicated dry slope conditions, more recent blast holes showed some water at their base which indicated the presence of water lower in the slope, perhaps transitional water holding up on the gouge zone on the fault. As such, water sensitivities were run on the dry back analysis model to test the effect of pore pressure on the stability margin. Three pore pressure conditions were chosen including a water table 15ft above the Pepperpike fault (created by duplicating the Pepperpike fault surface, converting to a water table surface and raising it 15ft above the fault), 10ft above the Pepperpike fault, and an Ru coefficient of 0.05. The Ru coefficient simply models the pore pressure as a fraction of the vertical earth pressure based on failure surface depth (Rocscience, 2022). These water cases did not represent a significant amount of water, and the resulting stability margins are presented in Table 3.

Given the limited amount of water observed in the field at this time, the 10 ft water table was initially chosen as the representative pore pressure case for back analysis. Figure 11 presents the alignment of critical slip surface found in this case compared to the radar sub-sampling, showing good correlation to the zones of highest movement (black dots).

Table 3. Back analysis iterative model runs and corresponding Factors of Safety.

Case	**Factor of Safety**
Dry Case	1.13
Ru=0.05	1.06
15ft water table on Pepperpike	1.05
10ft water table on Pepperpike	1.08

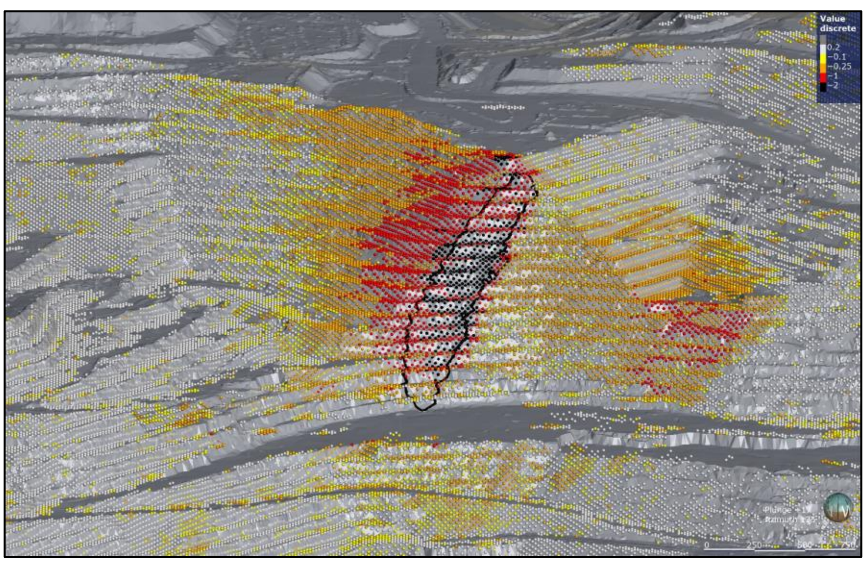

Figure 11. Initial back analysis results for 10 ft of constant head on the Pepperpike fault yielding a FS=1.08. Outline generated from Slide3 model result. Figure shows sub-sampled radar data alignment with the outline of the 3D slip surface.

The toe elevation used in the back analysis model was on the 5890 level, the active mining elevation when deformation rates took a step change. As successive benches were mined below this elevation visual seeps in the wall and regular saturated blast holes were increasingly observed. As a consequence, additional sub-surface monitoring instruments were installed, and horizontal depressurization holes were drilled. The field measurements were used to develop an updated “field-fit” water table, a schematic of which is shown in Figure 12. The field-fit water table represents a dry upper slope with water appearing in the lower elevations where the clay gouge fault infill exists.

The back analysis model was re-run with the field-fit water table and the stability results are shown in Figure 13. The field-fit water table shows slightly higher FS (at 1.09) than the 10ft water table case (1.08) due to removal of 10ft of water in the higher reaches of the Pepperpike fault, though it is likely more representative given it respects field hydrogeological observations. An additional “stretch” sensitivity was tested to observe the FS for the field-fit water table merged with 10 ft of head on the Pepperpike. Interestingly this gave a similar FS to the Ru=0.05 case. Given that the field-fit water table case met the target FS for the back analysis assessment, this became the new back analysis model which was used for predictive modeling.

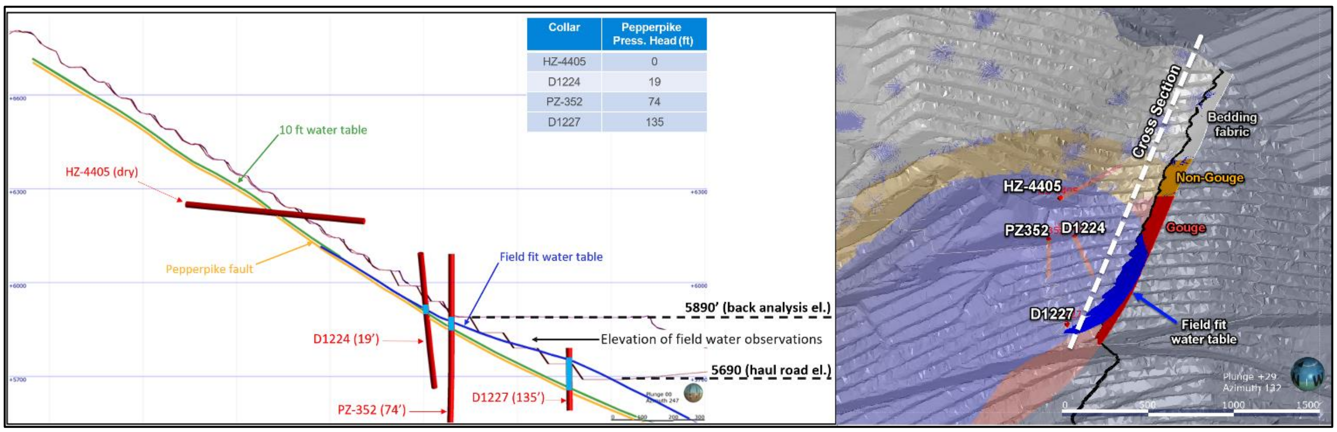

Figure 12. Schematic of the field-fit water table from monitoring data.

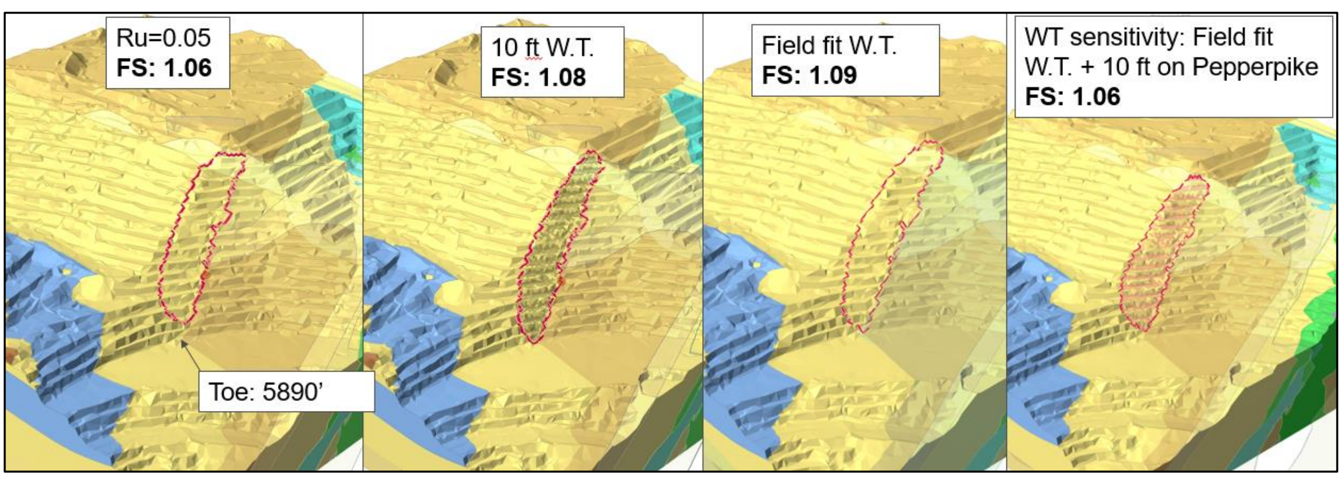

Figure 13. Pepperpike back analysis pore pressure sensitivities.

7 Predictive analysis and mitigation options

As part of economic risk assessment, the existing mine design and various mitigation alternatives were reviewed using the predictive stability model to assess options for reducing the risk of slope failure. These models included:

- Unload
- Buttress
- Depressurization

A 22Mt unload option was developed to remove driving force from the top of the critical geometry. This would carry significant cost to the mine plan from increased stripping and relocation of mine infrastructure. A 2.6Mt buttress option was developed to increase the resisting force at the toe of the critical mechanism. Longer-term mine plans would require removal of this buttress to develop a future mining cut in this area, so this solution would defer risk (and rehandling of the buttress material) to the future, as well as introducing rockfall hazards to operational areas below. All the predictive models did not include the effects of the depressurization program on the water table and thus presented slightly conservative results. Operations had already mobilized a horizontal rig that had drilled 34 depressurization holes by this time and had an ongoing depressurization programmed planned for successive benches.

Figure 14 presents the stability results for the existing mine design (no change going forward and no depressurization) and the conceptual unload option, with water table sensitivity. If mining continued to the existing plan, then the FS would reduce from 1.09 to 1.04, however it would toe out on the ramp that was planned to run 200ft below the toe of the back analysis mechanism. This indicates that the mechanism would grow as we mined down four more benches (200ft), but the ramp showed potential to decouple this mechanism. The 22Mt unload case would result in an increase in FS to 1.14 (+0.05), or for the water sensitivity case to 1.13 (+0.07). That is a significant unload for a relatively marginal increase in FS.

Figure 15 shows the stability results for the buttress case for both the field-fit water table and the water table sensitivity. The buttress material was given nominal Mohr-Coulomb strengths often used for simplified waste dump analysis of ϕ=37˚, c=0psf, since the angle of repose of the waste dumps is 37°. For a buttress constructed up to the 6090 level, the global minimum FS increased to 1.18 (+0.14).

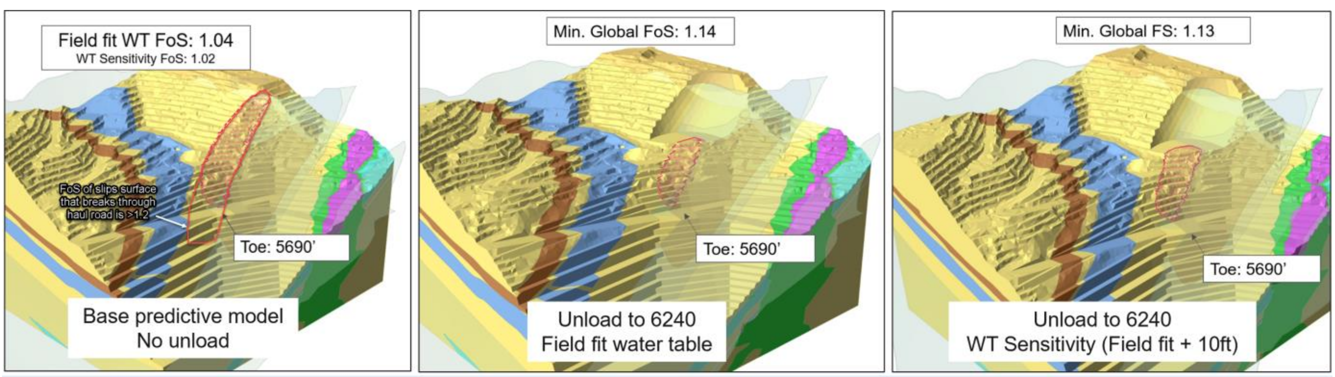

Figure 14. Predictive case with remediation option of unloading the slope from the crest.

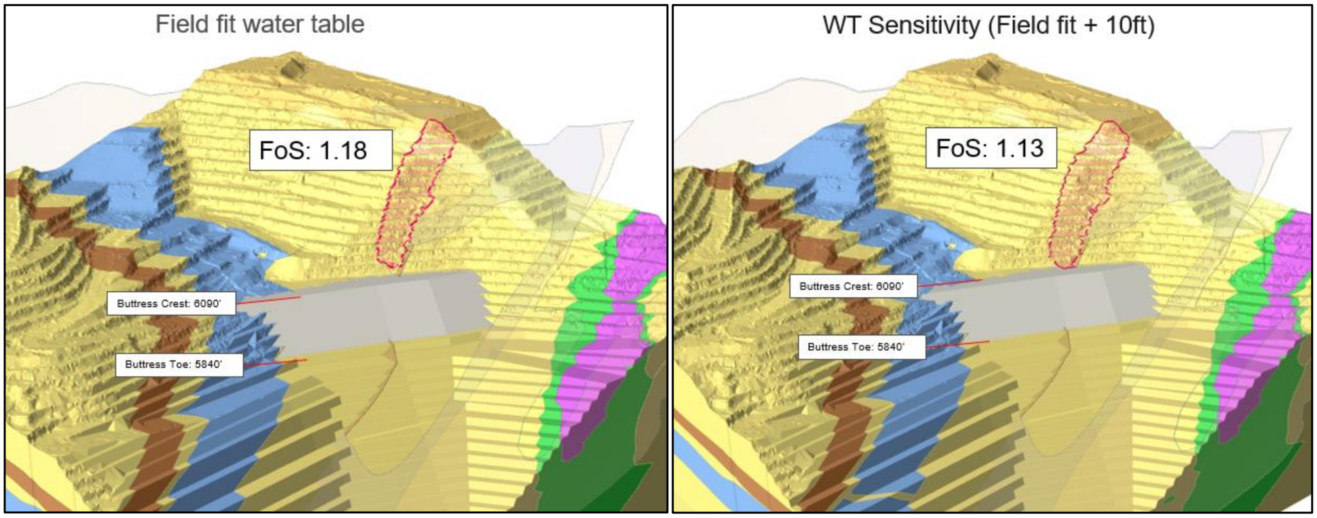

Figure 15. Predictive cases with remediation option of adding toe support and resistive load via a dumped in buttress.

8 Conclusions

The characterization, back analysis and predictive modeling of the Upper Ohio in 3D indicated that the instability mechanism would marginally grow down to the elevation of the haul road, but that the haul road would decouple the instability from continued mining on this wall. Further to this, an aggressive depressurization program was already underway to reduce pore pressures in the toe of the movement area. Under the controls of an observational mining approach discussed below, it was decided to continue mining to the current mine plan without immediately taking one of the remediation options. The remediation option remained available should the Upper Ohio reactivate. The area of deformation has since returned to background rates and the slope has responded well to depressurization efforts and observational mining.

The observational mining approach has been used successfully at Bingham Canyon mine for mining below an area of deformation with marginal stability and an FS less than the original Design Acceptance Criteria. The basis of observational mining is to closely observe the walls response to mining and adjust mining decisions based on that response. Key to this is accepting the risk that the original mine plan may likely need modification and accepting the associated economic uncertainty. Exploring this approach in detail is not within the scope of this paper, but generally involves:

- a detailed review of critical stability controls,
- assessment of probable conditions, possible deviations and associated responses,
- development of a robust monitoring program, an ongoing in-depth review of long- and short-term deformation trends with gate checks to document and approve mining progression,
- operational mining controls (wall control blasting, mining tonnage caps etc.) within an identified critical zone at the toe of the slope.

9 Lessons Learned

Key learnings from the development of the first major in-house 3D model at RTK model were:

- In-house modelling increases efficiency and agility, facilitating faster turnaround of results that enables timely input into mine planning decision-making, allowing opportunity to reduce production loss.
- The model inputs and uncertainties should already be well understood by the engineers, can be easily field checked, and ultimately the risk is owned by the in-house team.

- The selection of the slope stability assessment method (kinematic vs LE vs numerical) is important. More sophisticated and time-consuming assessment methods may not be beneficial if their complexity does not add necessary value.
- It is important to review multiple scenarios, investigate sensitivities, and involve multiple technical teams (Mine Planning, Geology, Hydrology, Hydrogeology, and Design and Operational Geotechnical Engineers) to ensure the model is most representative.
- Iterative refinement of model assumptions throughout the process is critical to maintain confidence in the results, particularly when new monitoring data or field observations become available as mining progresses, or the instability develops.

In summary, the upskilling and resourcing of in-house mine geotechnical engineers to carry out slope stability modelling has the potential to offer significant value to the Operation. External review of the technical data and modelling results is, however, very important in order to remain objective and develop robust solutions.

10 Acknowledgements

The authors would like to acknowledge the contributions of the Rio Tinto Kennecott technical, operational, and execution teams in the early identification of the Upper Ohio slope movement, its characterization, and the successful management of the hazard. A number of internal and external technical reviewers were also instrumental in contributing to the model development and interpretation of results which is further acknowledged by the authors.

11 References

Bar, N., Weekes, G. (2017). Directional shear strength models In 2D and 3D Limit Equilibrium analyses to assess the stability of anisotropic rock slopes in the Pilbara region of Western Australia. *Australian Geomechanics Society*, vol. 52, pp. 91-104.

Bar, N., Yacoub, T., McQuillan, A. (2019). Analysis of a large open pit mine in Western Australia using finite element and limit equilibrium methods. *Proceedings of the 53rd US Rock Mechanics/Geomechanics Symposium, New York.*

Kabuya, J., M., Simon, R., Carvalho, J., Haviland, D. (2020). Numerical back-analysis of highwall instability in an open pit: a case study. *Slopes Stability 2020, Perth*: pp. 937-952.

McQuillan, A., Yacoub, T., Bar, N., Coli, N., Leoni, L., Rea, S., Bu, J. (2020). Three-dimensional slope stability modelling and its interoperability with interferometric radar data to improve geotechnical design. *Slopes Stability 2020, Perth*: pp. 1349-1358.

Porter, J., Schroeder, K., Austin, G. (2012). Geology of the Bingham Canyon Porphyry Cu-Mo-Au Deposit, Utah. *Society of Economic Geologists 2012*: pp. 127-146.

Read, J. (2021). Three-dimensional limit equilibrium slope stability analyses, method, and design acceptance criteria uncertainties. *Slopes Stability 2021, Perth*: pp. 3-10.

Read, J., Stacey, P 2009, Guidelines for open pit slope design, CSIRO Publishing, Collingwood.

Rocscience Inc. 2022, SLIDE3, computer software, Rocscience, Toronto, https://www.rocscience.com/software/slide3